

1 **Experimental Investigation of the Energy Performance of a Novel Microencapsulated** 2 **Phase Change Material (MPCM) Slurry Based PV/T System**

3

4 Zhongzhu Qiu^{1,2}, Xiaoli Ma¹, Xudong Zhao^{1,*}, Peng Li³, Samira Ali⁴

5

6 ¹School of Engineering, University of Hull, Cottingham Road, Hull, UK

7 ²School of Energy & Mechanical Engineering, Shanghai University of Electric Power, Shanghai,
8 China

9 ³School of Mechanical Engineering, Tongji University, Shanghai, China

10 ⁴ Institute of Energy and Sustainable Development, De Montfort University, UK

11

12 **Corresponding email: Xudong.Zhao@hull.ac.uk*

13

14 **Abstract:** Based on the theoretical works completed by the authors, the paper presents an
15 experimental investigation into the energy performance of a novel PV/T thermal and power
16 system that employs the Micro-encapsulated Phase Change Material (MPCM) slurry as the
17 working fluid. A prototype PV/T module with the dimension of 800 mm × 1600 mm × 50mm was
18 designed and constructed based on previous theoretical modelling data. The performance of the
19 PV/T module and associated thermal and power system were tested under various solar radiations,
20 slurry Reynolds numbers and MPCM concentrations. It was found that (1) increasing solar
21 radiation led to the increased PV/T module temperature, decreased solar thermal & electrical
22 efficiencies and reduced slurry pressure drop; (2) increasing the slurry Reynolds number led to the
23 increased solar thermal & electrical efficiencies, decreased module temperature, and increased
24 pressure drop; and (3) increasing the MPCM concentration led to the reduced module temperature
25 and increased pressure drop. The experimental results were used to examine the accuracy of the
26 established computer model, giving a derivation rate in the range 1.1% to 6.1% which is an
27 acceptable error level for general engineering simulation. The optimum operational condition and
28 performance of the PV/T system could be outlined in such way: MPCM slurry weight
29 concentration of 10%, Reynolds number of 3,000, solar radiation of 500 W/m² to 700 W/m², and
30 the net overall solar efficiencies in the range 80.8% to 83.9%. To summarise, the MPCM slurry
31 based PV/T thermal and power system is superior to conventional air-sourced heat pump systems
32 (ASHP) and solar assisted heat pump systems (ISAHP), and has the potential to help reduce fossil
33 fuel consumption and carbon emission to the environment.

34

1 **Key words:** Experimental investigation; Energy performance; MPCM slurry; PV/T module;
 2 Thermal and electrical efficiencies; Concentration

3

Nomenclature			
A	Module area, m^2	S_e	standard deviation of the groups of testing results
C_p	Specific heat capacity, $kJ \cdot kg^{-1} \cdot K^{-1}$	w	Weight concentration
D	Diameter, m	x_e	the experimental
I	Solar irradiance, W/m^2	x_s	simulation value
K	Thermal conductivity, $W \cdot m^{-1} \cdot K^{-1}$	\bar{x}_e	arithmetic mean experimental value
\dot{m}	Mass flow rate, kg/s		
n	The number of experiments implemented	Greek symbol	
Q_{pump}	Pump electricity consumption, W	ρ	Density, $kg \cdot m^{-3}$
Q_{th}	Heat output, W	μ	Dynamic viscosity, $Pa \cdot s$
Q_e	Electricity output, W	η_e	Electrical efficiency
$RMSPE$	Root mean square percentage error	η_{th}	Thermal efficiency

4

5 **1. Introduction**

6

7 Solar energy technology is regarded as one of the most mature renewable technologies for heating
 8 and/or power generation which, by 2030, expects to provide nearly 50% of low and medium
 9 temperature heat ^[1] and 5% of total electricity demand ^[2] within the EU. The PVs is currently the
 10 most popular solar power device that has the temperature-dependant solar electrical output.
 11 Increasing temperature of the PV cells by 1°C would lead to 0.5% reduction in solar electrical
 12 efficiency for the crystalline silicon cells and around 0.25% for the amorphous silicon cells ^[3, 4].
 13 To control the temperature of the cells, several measures were applied to remove the accumulated
 14 heat from the rear of the PV modules and further to make good utilization of the removed heat.
 15 This approach, known as the PV/Thermal (PV/T) technology, has been proven to be effective in
 16 increasing the system's solar efficiency and making economic use of solar energy.

17

18 During the operation, the dedicate PV/T modules convert one part of the incident solar radiation
 19 into electricity by means of photo-electronic effect of the PV cells and another part of incident

1 solar radiation into heat by means of heat transportation characteristics of the working fluid,
2 thereby providing an enhanced overall energy efficiency than conventional PV panels. The use of
3 air, water, or refrigerants as the heat transportation fluid in the PV/T systems has been fully
4 investigated [5-8], thus delivering several important conclusions: (1) air has poor heat removal
5 effectiveness owing to its lower density, specific heat and thermal conductivity [5]; (2) compared to
6 air, water has the enhanced heat removal performance but its effectiveness is limited by the
7 cycling temperature [6]; (3) a refrigerant, e.g., R401, owing to the change in phase leading to
8 significant latent heat absorption at a low and fixed temperature, has significantly enhanced heat
9 removal performance. However, use of a refrigerant faces several practical challenges, i.e., high
10 risk of refrigerant leakage and uneven refrigerant flow/distribution across the multiple coils in a
11 large area [7, 8].

12
13 A MPCM slurry is such a kind of solution comprising the dispersing micro-particles that are
14 encapsulated by the polymer shells ranging from 1 to 1000 μ m and a carrier fluid (e.g. water) that
15 is mixed with the selected additives [9]. As a new functional thermal fluid, the MPCM slurry has a
16 higher thermal capacity over the conventional single phase heat transportation fluids, owing to the
17 engagement of the latent heat resulted from the phase change, thus creating the enhanced heat
18 transfer rate and increased heat storage capacity [10].

19
20 Although the MPCM slurries have been well used in HVAC systems as the heat transportation and
21 heat storage media, the use of such slurries in PV/T systems has not yet been reported except the
22 authors' preliminary study delivered in ref [11], which presented the theoretical study of the
23 performance of a novel MPCM slurry based PV/T system. As a follow-on work, this paper
24 presents the experimental investigation of the operational performance of such a system that
25 would provide the validation, examination and update to the established theory and computer
26 model. From this point of view, the research will help develop an innovative PV/T technology
27 employing the MPCM slurry as a working fluid and enabling the enhanced solar efficiency, thus
28 contributing to significant fossil fuel energy saving and carbon emission reduction globally.

29

30 **2. The novel PV/T module and MPCM slurry**

31

32 **2.1 The novel PV/T module**

33

1 A novel PV/T module was designed and constructed based on previous modelling work^[11]. The
2 configuration of the module is shown in **Fig. 1**. This module has a multi-layer structure that
3 comprises the following components:

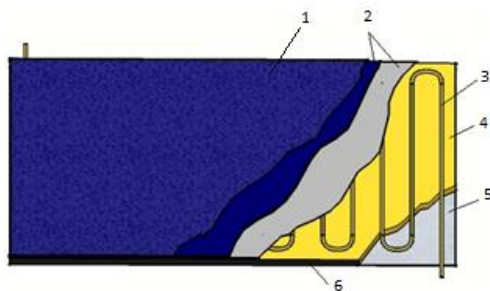
- 4
- 5 1) Back layer - a light-weight reinforced polystyrene board;
- 6 2) Insulation layer - a 40 mm mineral wool;
- 7 3) A copper serpentine tube layer;
- 8 4) A PV module layer;
- 9 5) Outer cover layer;

10

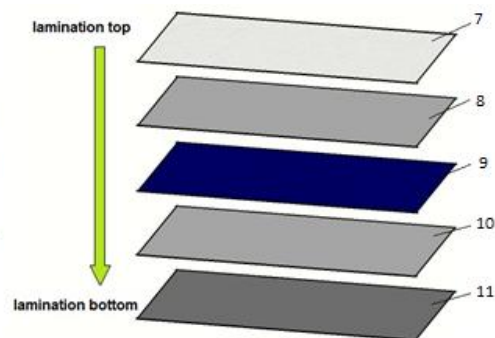
11 The copper serpentine tube, which is attached to the back surface of the module, allows the PCM
12 slurry to flow across, during which time the phase change of the PCM particles will take place.
13 Owing to the melting of the micro-encapsulated PCM particles occurring in the flowing slurry
14 which involves the latent heat absorption, a higher heat transfer rate will be achieved during this
15 process, leading to the reduced PV module temperature and the increased module solar electrical
16 efficiency. The PV module layer, which incorporates numerous PV cells connected in parallel or
17 in series, is laminated on a thermally-conductive base sheet. This layer, adhering to the serpentine
18 tube layer, will convert part of solar radiation into DC power and conduct the remaining solar heat
19 from the PV cells to the serpentine tube. The outer cover layer is a clear glazing with very high
20 solar transmittance (above 0.9) which will allow transmission of the solar radiation and prevent
21 excessive heat loss from the module surface. These layers together form an integrated module
22 generating the DC current which, via the inverter, will be converted into the AC current and
23 delivered into the grid or battery storage.

24

25



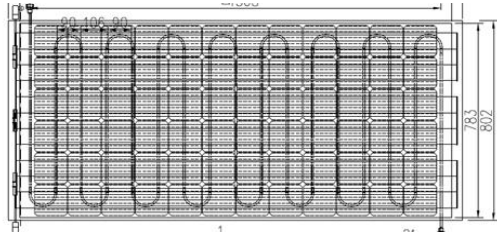
26
27 (a) The module



(b) The configuration of PV lamination

1 Covered glass (corrected to here), 2 PV lamination, 3 Absorb pipe, 4 Thermal insulation, 5 Frame
 2 base, 6 Frame set, 7 Tempered glass, 8 EVA sealant, 9 PV cell, 10 EVA sealant, 11 Aluminium
 3 alloy plane

4 **Fig. 1** The module and configuration of the PV lamination



6
 7 *Fig. 2 Schematic of a single module's*
 8 *serpentine absorb pipe design*



9
 10 **Fig. 3** The module photograph

11 The geometrical, thermal and physical parameters in relation to the prototype module are detailed
 12 in **Table 1**.

13 **Table 1.** The geometrical, thermal and physical parameters of the module

Item	Value
<i>Dimension</i>	
PV/T module area, m ²	1.28
PV electricity net area, m ²	1.177
Absorb tube inner diameter, m	0.007
Absorb tube outer diameter, m	0.09
Tube spacing, m	0.095
Thickness of PV cell, mm	0.2
Thickness of tempered glass layer in lamination, mm	3.2
Thickness of EVA layer, mm	0.50
Thickness of bond, mm	10
Thickness of aluminium alloy plane, mm	1
Thickness of insulation, mm	40
Thickness of back plate, mm	10
<i>Thermal conductivity</i>	
Thermal conductivity of absorber(copper), Wm ⁻¹ K ⁻¹	390
Thermal conductivity of PV cell, Wm ⁻¹ K ⁻¹	84
Thermal conductivity of glass, Wm ⁻¹ K ⁻¹	1.0

Thermal conductivity of EVA, $\text{Wm}^{-1}\text{K}^{-1}$	0.35
Thermal conductivity of bond, $\text{Wm}^{-1}\text{K}^{-1}$	1.15
Thermal conductivity of aluminium alloy, $\text{Wm}^{-1}\text{K}^{-1}$	230
Thermal conductivity of insulation, $\text{Wm}^{-1}\text{K}^{-1}$	0.045
Thermal conductivity of polystyrene board, $\text{Wm}^{-1}\text{K}^{-1}$	0.39
<i>Others</i>	
Cell's electrical efficiency at reference temperature, %	16.5
Temperature coefficient of PV cell power generation	0.0045
Module electricity output at rated condition, W	195

1

2 **2.2 The MPCM slurry and its properties**

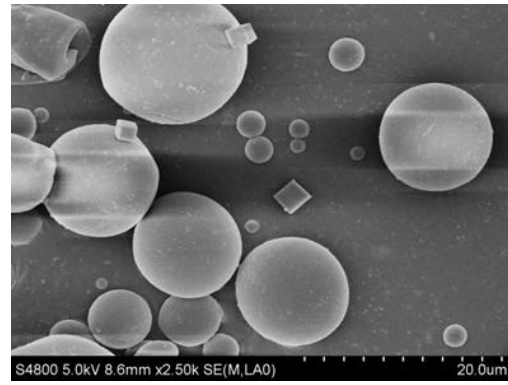
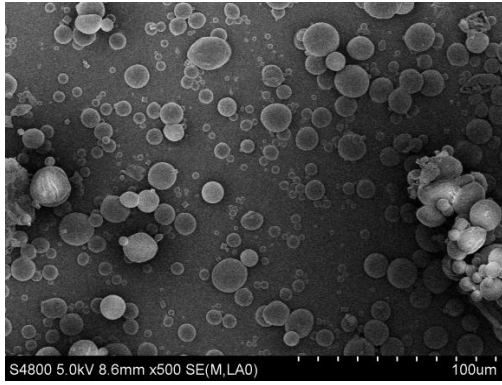
3

4 The paraffin is a chemically stable phase change material (PCM) that could remain fairly steady
5 thermal performance during a long term operation. The micro-encapsulated phase change material
6 (MPCM) used in the experimental system is made of paraffin which was wrapped by the polymer
7 shells. A range of commercial available paraffin MPCMs were investigated in terms of their
8 operational scope and suitability for the experimental PV/T module system. The MPCM-28,
9 provided by the Microtech Laboratories Inc ^[12] of USA, was selected for the use in the
10 experimental system.

11

12 The morphology of the micro-encapsulated PCM was observed using a Scanning Electron
13 Microscope (SEM) instrument (JEOL JSM- 6400, Japan). **Fig. 4** shows the images of the micro-
14 capsules for different instrument magnification. It is shown that the micro-capsules have smooth
15 and spherical surfaces. The diameters of microcapsules were measured by a particle
16 characterization system (Malvern Instrument, Malvern Masterzer 2000). It was found that the
17 micro-encapsulated PCM particles have the diameters ranging from 1 to 100 μm , with the average
18 diameter of 18.2 μm , as shown in **Fig. 5**.

19



(a)1:500

(b)1:2500

Fig. 4 SEM images of MPCM particles for different magnification

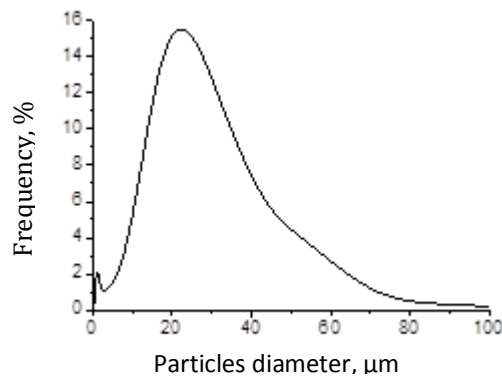


Fig. 5 Diameter of the MPCM particles

Water and the MPCM particles were mixed at the weight ratios of 95:5, 90:10 and 85:15 respectively to produce MPCM slurry with different concentrations, i.e., 5%, 10% and 15% in weight. A small amount of additives was added to the slurry to enhance its stability and fine dispersion. The samples of the prepared slurries are shown in **Fig. 6**.



(a) Physical stability experiment



(b) Flow ability

Fig. 6 Appearance of the prepared slurry

1 The thermal and physical properties of the selected MPCM capsule and its slurry were shown in
 2 **Table 2**. The viscosity data of the slurry, which were measured using rheometer Physica MCR
 3 102 (Anton Paar), are presented in **Table 2**; while other properties, calculated by using the
 4 relevant correlations, are also presented in **Table 2**.

5
6

Table 2. Thermal and physical properties of a MPCM slurry and its components

	Density $kg \cdot m^{-3}$	Specific Heat $J \cdot kg^{-1} \cdot K^{-1}$	Thermal Conductivity $W \cdot m^{-1} \cdot K^{-1}$	Latent Heat $kJ \cdot kg^{-1}$	Viscosity $mPa \cdot s$ At 298 K
Paraffin(Solid)	849	1800	0.358	244	-
(Liquid)	806	2200	0.148		
Polymer	1490	1670	0.42	-	-
Water(at 298 K)	997	4180	0.61	-	0.87
MPCM	899.9	1779	0.34	213.5	-
particle(Solid)					
(Liquid)	854	2135	0.14		
MPCM Slurry*					
(Weight concentration w)					
w = 0.05	992	4060	0.594	10.7	1.08
w = 0.10	986	3940	0.579	21.4	1.28
w = 0.15	980	3824	0.564	32.1	2.23

7 *Bulk physical properties of slurries shown here are calculated using those of the solid MCPCM particles.

8

9 The equations for calculating the density and specific heat of different micro-capsules and relevant
 10 slurries can be derived on the mass and energy balance principle ^[13, 14], given by

11

$$12 \quad \rho_{particle} = \left(\frac{D_{core}}{D_{particle}} \right)^3 \frac{\rho_{core}}{w_{core}} \quad (1)$$

13

$$14 \quad C_{p,particle} = \frac{(w_{core} \cdot C_{core} + w_{shell} \cdot C_{shell}) \rho_{core} \rho_{shell}}{(w_{core} \cdot \rho_{shell} + w_{shell} \cdot \rho_{core}) \rho_{particle}} \quad (2)$$

15

$$16 \quad C_{p,slurry} = w_{particle} C_{p,particle} + w_{water} C_{p,water} \quad (3)$$

17

1 The thermal conductivity of the micro-capsule was calculated using the composite sphere
 2 approach ^[15], given by:

$$3 \frac{1}{K_{particle} D_{particle}} = \frac{1}{K_{core} D_{core}} + \frac{D_{particle} - D_{core}}{K_{shell} D_{particle} D_{core}} \quad (4)$$

5
 6 The thermal conductivity of the MPCM slurry was calculated using the Maxwell's relation ^[16],
 7 given by

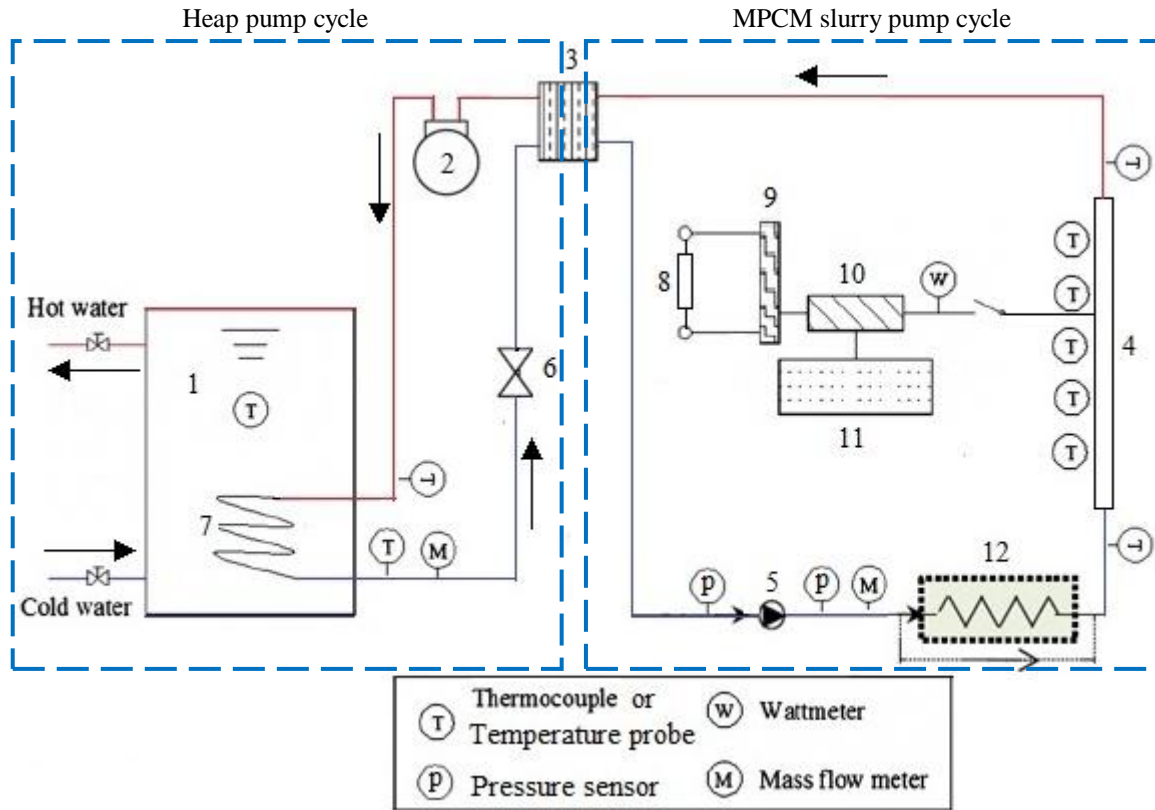
$$8 \quad 9 \quad K_{slurry} = \frac{2K_{water} + K_{particle} + 2w_{particle}(K_{particle} - K_{water})}{2K_{water} + K_{particle} - w_{particle}(K_{particle} - K_{water})} \quad (5)$$

10 **3 Experimental testing system**

11 12 **3.1 Configuration of the experimental system**

13 **Fig. 4** shows a schematic of the experimental system. The system is comprised of a PV/T module,
 14 a slurry-to-refrigerant heat exchanger (evaporator), a compressor, a refrigerant-water heat
 15 exchanger (condenser), a water tank, an inverter, and other necessary accessories including a
 16 slurry pump, the valves, an electrical resistance and a controller. During the operation, the PV/T
 17 module (4) will absorb “solar radiation” illuminated from a solar simulator; part of which will be
 18 converted into electricity by means of the PV cells and the second part converted into heat. The
 19 heat generated within the PV cells will be taken away by the MPCM slurry flowing across the
 20 serpentine piping attached on the back surface of the PV cells. This amount of heat will be
 21 absorbed by the slurry and cause the MPCM particles in the slurry to melt, thus leading to a
 22 reasonably low temperature rise during the phase change process. The slurry will then flow into
 23 the evaporator of the heat pump, i.e, the slurry-to-refrigerant heat exchanger (3), where the heat
 24 transfer between the MPCM slurry and the working fluid (R134a) in the heat pump loop will take
 25 place, leading to ‘frozen’ of the MPCM particles within the slurry and evaporation of the
 26 refrigerant (R134a) of the heat pump cycle. The heat pump cycle will rise the refrigerant
 27 temperature from around 15 °C to 70 °C, depending the requirement of the heating system. The
 28 heat in the refrigerant will be released to passing water in the condenser, thus generating domestic
 29 hot water for the use in buildings. The condensed refrigerant will then return to the evaporator via
 30 an expansion valve to complete the cycle. An electrical pre-heater (12) will be used to regulate the
 31 temperature of the MPCM slurry at the inlet of PV/T module to create a stable operational

1 condition. A charge controller (10) will provide a regulated DC output which is used to power the
 2 DC equipment (4), stores excess energy into a battery (11), as well as monitor the battery voltage
 3 to prevent under/over power charging. An inverter (9) will be connected to the charge controller to
 4 convert the DC power to AC type, which is used for powering the AC load (8).



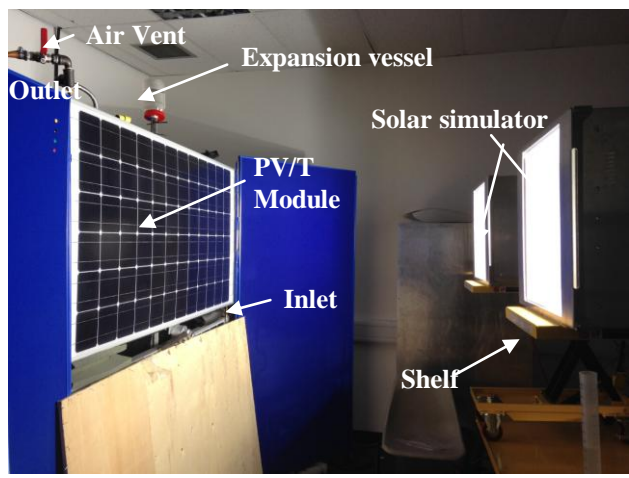
1-water tank; 2-Compressor; 3-Slurry-refrigerant heat exchanger (evaporator); 4-PV/T module; 5- Pump;
 6- Expansion valve; 7- Refrigerant-water coil(condenser); 8- Resistance; 9- Inverter; 10- Controller; 11-
 Battery ; 12- Re-heater for inlet temperature regulation

Fig. 4 The experimental system

3.2 Experimental system setting up

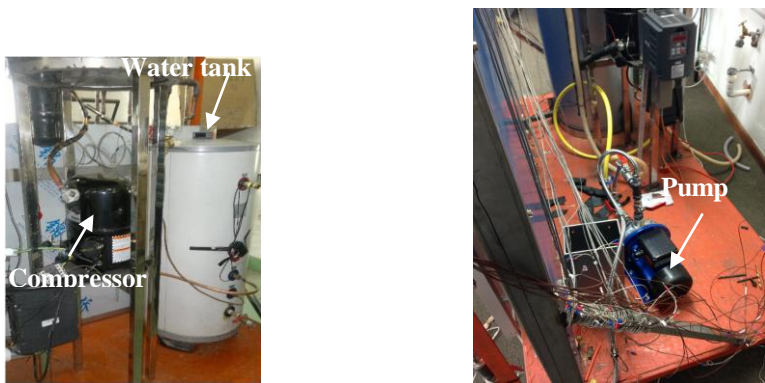
The experimental prototype system was constructed and the testing system was developed at the Energy Technologies Laboratory in University of Hull. Commercially available components were used to construct the prototype system. These include a compressor (Tecumseh, FH4518Y) and a pump (CEAM70/5-V/A, Xylem) that are shown in **Figs. 5** and **6** respectively. Two solar simulators (SolarConstant 4000 Radiation unit Inclusive 4000W lamp and UV-Filter (Atlas)) are positioned at 1.2m away from the PV/T module, enabling the module to receive solar radiation in a convenient way.

1 The experimental system was monitored and measured during the operational process. The
2 measurement instrument assembly and installation are shown in **Fig. 4**. The temperature, pressure
3 and flow rate were measured using the thermocouples/temperature probes, pressure transmitters
4 and flow sensor respectively. A power meter was used to measure the PV/T module power output.
5 The outputs of the sensors could be transmitted into a Data Logger and then to the computer. The
6 irradiance of the solar simulator was measured by means of a pyranometer. Furthermore, a particle
7 analyser was used to measure MPCM particle size and a Rheometer was used to measure the
8 viscosity of MPCM slurry during the experimental process. The specification, quantity and
9 installation position of the sensors/meters used in the measurement process are outlined in **Table**
10 **3**.



11
12
13
14

Figure 5 Front view of the experimental system



15
16
17
18
19
20

Figure 6 Back view-components in the experimental system; (a) Compressor and water tank (b) Pump

1

Table 3. Main experimental instruments for measuring parameters

Instrument/Device	Specification	Quantity	Measurement points
Solar simulator	SolarConstant 4000 Radiation unit Inclusive 4000W lamp and UV- Filter(Atlas)	2	In front of the module
Pyranometer	LP02-TR (Hukseflux)	1	On the bracket of the module.
Power sensor	WB1919B35-S and WBP112S91 (Weibo, China)	1	Module power output (DC)
Pressure Transmitter	3100R0010G01B000,10bar, 0- 5V(Germs Sensors)	2	Inlet and outlet of the module
Flow sensor	200psi Pressure, 0.5-5 (Germs Sensors)	2	Inlet and outlet of the module
Thermocouples	T type	15	Module's backplane
Temperature Probes (RTD)	PT100 RTD probes 90/00543945(Jumo, UK)	2	module's inlet/outlet (slurry side), liquid line
Particle analyser	Malvern Masterzer 2000 (Malvern Instrument)	1	MEPCM particle size measurement
Rheometer	Physica MCR 102 (Anton Paar)	1	For measuring viscosity of the MPCM slurry
Data logger	Agilent - 34972A&2 A3901 terminal modules(Agilent technologies)	1	Record data with computing unit

2

3 4. Experimental testing methodology

4

5 The laboratory testing was carried out at the Energy Technology Laboratory, University of Hull,
6 from 10 Jun 2014 to 12 Jul 2014. All the sensors/meters were calibrated by following the relevant
7 standards. Tests were carried out to investigate the impact of solar radiation (I), MPCM slurry
8 flow condition (Re) and MPCM slurry concentration (w) onto the performance of the PV/T
9 module. To enable this, tests were carried out under various operational conditions, detailed below:

10

- 11 (1) Solar radiation (I) varying from $500(\pm 5)$ to $900(\pm 5)$ W/m^2 when keeping all other
12 operational parameters constant.
- 13 (2) Slurry Reynolds number (Re) varying from 1,508 to 3,496 when keeping all other
14 operational parameters constant.

(3) MPCM slurry weight concentration (w) varying from 0%, 5% to 10% and solar radiation (I) varying from 500(± 5) to 900(± 5) W/m^2 , while all other operational parameters remained constant.

(4) Ambient temperature (T_a) was fixed to 29.5(± 1) $^{\circ}C$ throughout the measurement process.

(5) MPCM slurry temperature at the module inlet (T_i) was fixed to 24.75(± 0.5) $^{\circ}C$ throughout the measurement process.

In summary, three sets of tests were carried out and their operational parameters were outlined in **Table 4**.

Table 4. Test conditions

	$I, W/m^2$	Re	$W, \%$	$T_a, ^{\circ}C$	$T_i, ^{\circ}C$
Test 1	500 - 900	2910	10	29.5	24.75
Test 2	600	1508 - 3496	10	29.5	24.75
Test 3	700	3000	0 - 15	29.5	24.75

5 Results and discussions

The steady state solar thermal efficiency (η_{th}) of a conventional flat plate solar collector is expressed as:

$$\eta_{th} = \frac{Q_{th}}{IA} \quad (6)$$

Where, the collected useful heat (Q_{th}) is given by

$$Q_{th} = \dot{m}C_p(T_o - T_i) \quad (7)$$

The steady state solar electrical efficiency (η_e) of a conventional flat plate solar collector is expressed as:

$$\eta_e = \frac{Q_e}{IA} \quad (8)$$

The module net efficiency is defined as

$$\eta_{net} = \eta_e + \eta_{th} - \frac{Q_{pump}}{IA} \quad (9)$$

To enable a parallel comparison between the simulation and the testing results, the computer model was operated at the identical condition as the experiment did. To identify the discrepancy

1 between the measured and simulated results, the root mean square percentage error (RMSPE)
 2 were applied, given by

$$RMSPE = \sqrt{\frac{\sum_{i=1}^n [100 \times (x_{e,i} - x_{s,i})]^2}{n}} \quad (10)$$

3 The uncertainty of the experiment results is then correlated to the standard deviation

$$S_e = \sqrt{\frac{1}{n} \sum_{i=1}^n (x_{e,i} - \bar{x}_e)^2} \quad (11)$$

4 As a result, the uncertainty ratio of the experimental results can be written as

$$U = \frac{S_e}{\bar{x}_e} \quad (12)$$

5
 6 Where, n is the number of experiments implemented; x_e e and x_s xs are the experimental and
 7 simulation values, respectively; \bar{x}_e is the arithmetic mean experimental value. S_e is the standard
 8 deviation of the groups of testing results during each testing mode.

9

10 **5.1 Impact of the solar radiation**

11

12 Test 1 was carried out to investigate the impact of solar radiation onto the performance of the
 13 PV/T thermal and power system, based on the operational conditions listed in **Table 4**. The testing
 14 results were presented in **Figs. 7 to 11**. Meanwhile the data derived from the previously
 15 established computer model at the equivalent operational conditions, RMSPE, maximum
 16 uncertainty ratio (U_{max}), and mean uncertainty ratio (\bar{U}) were also presented in these figures to
 17 enable the parallel comparison between the testing and modeling.

18

19 It is seen from **Figs. 7 and 8** that increase in solar irradiation from 500W/m² to 900W/m² led to
 20 significant increase in the power output of the PV/T module (from 91.6 W to 157.0 W) and in its
 21 heat output (from 448.5W to 743.3W).

22

23 Variation of the module's back surface temperature against solar irradiation is shown in **Fig. 9**.
 24 When increasing the solar irradiation from 500W/m² to 900W/m², the temperature experienced a
 25 slow rise, from 32.4°C at the start time to 34.6°C at the finish time. The temperature rise scale was
 26 found to be much less than that in the water based PV/T system, owing to the phase change
 27 occurring in this process, which enabled the same amount of heat absorption with very low (near
 28 zero) temperature rise.

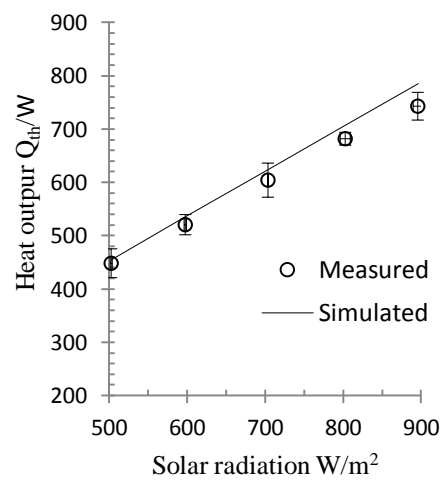
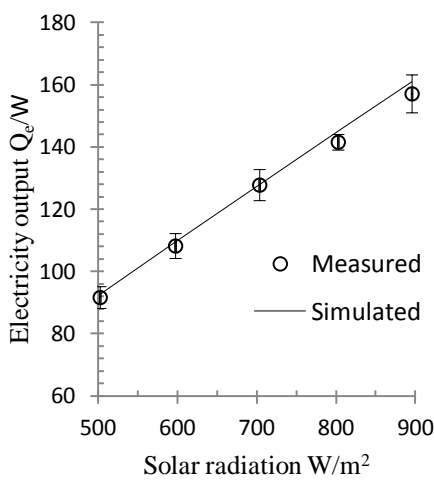
1
 2 Variation of the slurry's pressure drop across the serpentine tube against solar irradiation is shown
 3 in **Fig. 10**. When increasing the solar irradiation from 500W/m^2 to 900W/m^2 , the pressure drop
 4 fell from $29.4 \times 10^4\text{Pa}$ to $26.9 \times 10^4\text{ Pa}$. This indicates that the increasing solar irradiation helped
 5 reducing the slurry's flow resistance, owing to the increased slurry temperature and decreased
 6 viscosity during this process.

7
 8 **Fig.11** indicates that the module's net efficiency presented a downward trend ranging from 83.9%
 9 to 78.5% when solar radiation was on growth.

10
 11 **Figs 7 to 11** also presented the parallel comparisons between the modeling and experimental
 12 results which were justified by the maximum uncertainty ratio (U_{max}) and mean uncertainty ratio
 13 (\bar{U}). For all sets of testing, the U_{max} was in the range 3.3% to 12.4% with the average figure of
 14 10.6%. This derivation was possibly caused by a number of fluctuated parameters including air
 15 temperature, electrical voltage imposed on the compressor and pump, the slurry flow rate, as well
 16 as set-up of the thermocouples. The root mean square percentage deviation (RMSPE) was below
 17 6.1%, which was possibly caused by both (either) unrealistic theoretical assumptions and (or)
 18 measurement inaccuracies. When considering the uncertainties existing in the measurement, the
 19 validation results were acceptable for the general engineering applications. This indicated that the
 20 developed theoretical model by the authors ^[11] could predict the energy performance of the
 21 MPCM slurry based PV/T system at an acceptable accuracy.

22

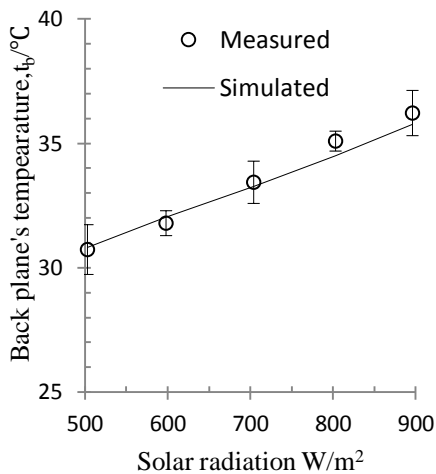
23



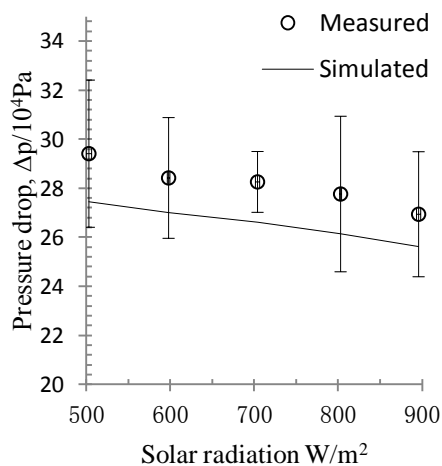
24 **Fig. 7** Module electricity output vs solar radiation
 25 (RMSPE=1.8%, U_{max} = 3.9%, \bar{U} = 3.4%)

Fig. 8 Module heat output vs solar radiation
 (RMSPE=3.5%, U_{max} = 6%, \bar{U} = 4%)

1



2



3

Fig. 9 Module temperature vs solar radiation

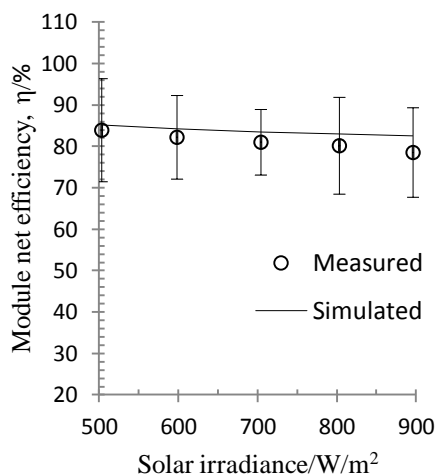
Fig. 10 Module pressure drop vs solar radiation

4

(RMSPE=1.1%, $U_{\text{max}}= 3.3\%$, $\bar{U} = 2.2\%$)

(RMSPE=6.1%, $U_{\text{max}}= 11.4\%$, $\bar{U} = 8.8\%$)

5



6

Fig. 11 Module net efficiency vs solar radiation

7

(RMSPE=3.2%, $U_{\text{max}}= 12.4\%$, $\bar{U} = 10.6\%$)

8

9

10

11

5.2 Impact of the slurry flow condition

12

13 Test 2 was carried out to investigate the impact of Reynolds number of the MPCM slurry flow
14 onto the performance of the PV/T system, based on the operational conditions listed in Table 4.

15 The testing results are shown in **Figs. 12 to 16**.

16

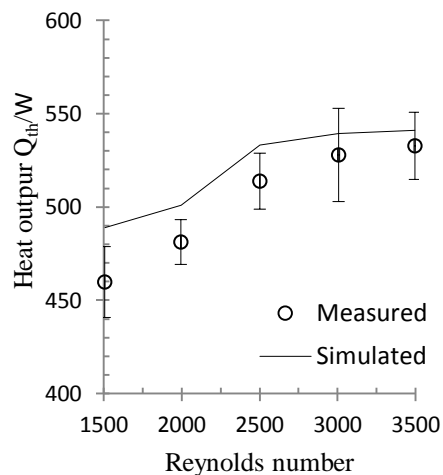
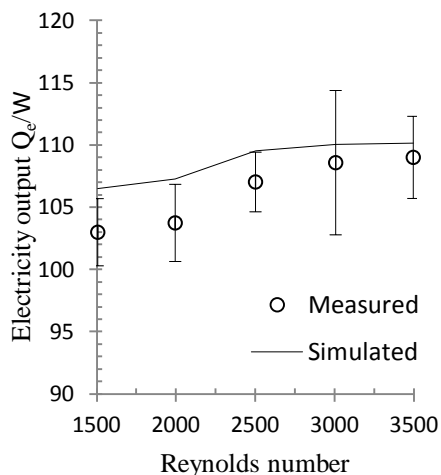
1 It is seen from **Figs. 12** and **13** that increase in Reynolds (Re) from 1508 to 3496 led to certain
2 increase in electrical output of the PV/T module (from 103 W to 108.6 W) and in its heat output
3 (from 460W to 528W). This indicates that higher Reynolds (Re) condition helped improve the
4 heat transfer between the slurry and PV cells, which subsequently enhanced the heat and
5 electricity outputs of the system.

6
7 Variation of the slurry's pressure drop across the serpentine tube against Reynolds number is
8 shown in **Fig. 15**. When increasing the Reynolds number from 1508 to 3496, the pressure drop
9 grew from 8.1×10^4 Pa to 44.5×10^4 Pa. The module temperature presented a downward trend when
10 the Reynolds number was on growth (**Fig.14**). This is because the growth in Reynolds number led
11 to the more heat being taken away by MPCM slurry, hence achieving the better cooling effect to
12 the PV/T module.

13
14 **Fig. 16** indicates the module's net efficiency increased from 73.1% to 81.6% when the Reynolds
15 number increased from 1,508 to 3,007, and afterwards, the net efficiency fell from 81.6% to 81.3%
16 when the Reynolds number increased from 3,007 to 3,496. This is because when the Reynolds
17 number grew to a certain level (i.e. around 3,000 in the case), slurry flow resistance across the
18 serpentine pipe quickly grew and became the dominant factor impacting on the performance of the
19 PV/T system. As a result, power consumption of the slurry pump grew significantly that led to the
20 change of the system's net efficiency variation from the upward to downward trend. In this
21 circumstance, the Reynolds number of 3,000 was considered as the optimum operational flow
22 state, as indicated in **Table 4**.

23
24 **Figs 12 to 16** also show the comparisons between the modeling and experimental results under
25 this set of operational condition. It was found that the U_{max} was in the range 3.3% to 12.7% with
26 the average figure of 9.6% while the root mean square percentage deviation (RMSPE) was below
27 5%. This indicates that the developed theoretical model by the authors ^[11] could predict the energy
28 performance of the MPCM slurry based PV/T system at an acceptable accuracy.

1



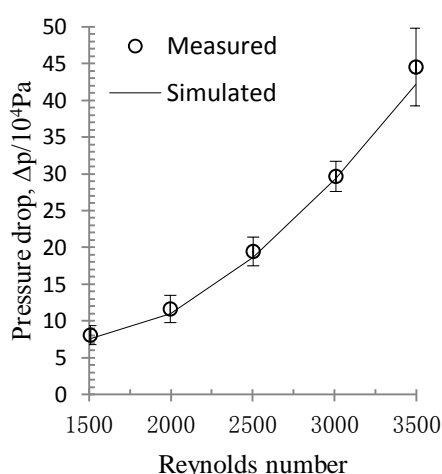
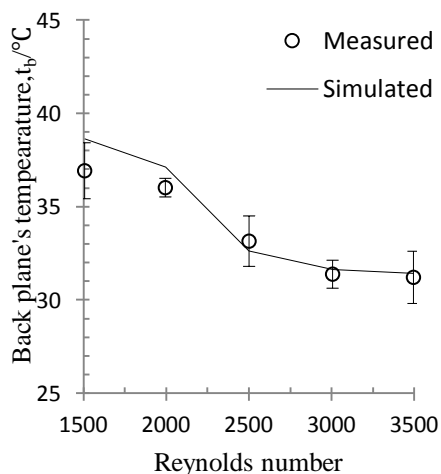
2

Fig. 12 Module electricity output vs. Reynolds number
(RMSPE=2.4%, U_{max} = 3.3%, \bar{U} = 2.8%)

Fig. 13 Module heat output vs. Reynolds number
(RMSPE=3.7%, U_{max} = 4.7%, \bar{U} = 3.5%)

3

4



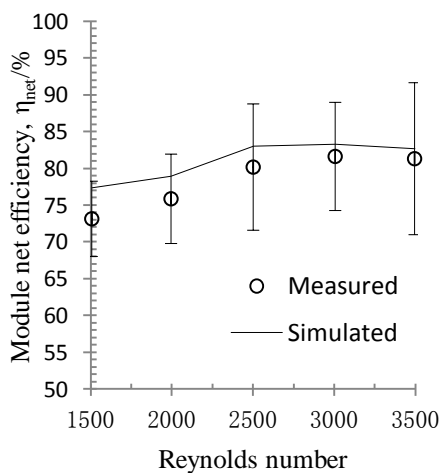
5

6

Fig. 14 Module temperature vs. Reynolds number
(RMSPE=2.5%, U_{max} = 4.5%, \bar{U} = 3.3%)

Fig. 15 Module pressure drop vs. Reynolds number
(RMSPE=5.0%, U_{max} = 11.9%, \bar{U} = 8.2%)

7



8

1 **Fig. 16 System's net efficiency vs. Reynolds number**

2 (RMSPE=3.6%, U_{max} = 12.7%, \bar{U} = 9.6%)

3
4 **5.3 Impact of the MPCM slurry concentration**

5
6 Test 3 was carried out to investigate the impact of the MPCM slurry concentration onto the
7 performance of the PV/T system, based on the operational conditions listed in Table 4. During the
8 test, the slurry weight concentration varied from 0% to 15%. The test results are shown in **Figs. 17**
9 **to 21**.

10
11 **Figs. 17 and 18** indicate that both heat and power outputs of the PV/T module increased with the
12 increase of the slurry concentration, presenting a near-to-linear trend of variation. **Fig. 19** indicates
13 that the module's surface temperature fell when increasing the slurry concentration; while **Fig. 20**
14 indicates that pressure drop of the slurry across the serpentine pipe increased with the increase of
15 the slurry concentration. In terms of the net power output, which is a figure of the PVs' power
16 output subtracted by the pump power consumption, the maximum figure occurred at the 10% of
17 slurry concentration.

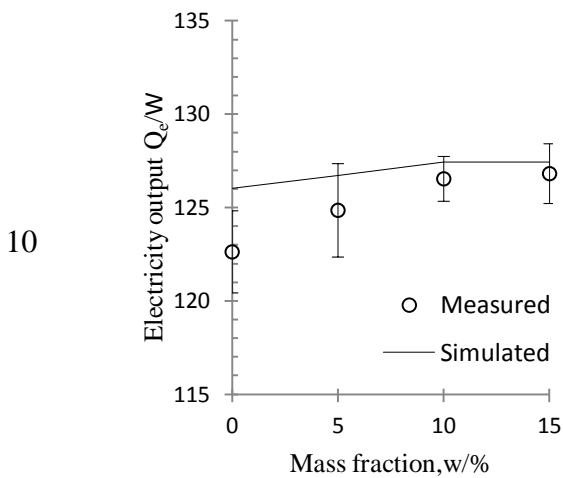
18
19 **Fig. 21** indicates that the module's net efficiency increased from 77.8% to 80.8% when the
20 MPCM's weight concentration increased from 0 to 10%. However, when the concentration
21 continued to grow (i.e., from 10% to 15%), the net efficiency of the module started to fall (from
22 80.8% to 78.2%). The reason for the change in variation trend was mainly caused by the viscosity
23 effect of the slurry. The high concentration was correlated to the high viscosity which
24 consequently led to the significantly increased slurry pump power consumption and decreased net
25 efficiency. From this point of view, the weight concentration of the MPCM slurry should remain
26 at around 10%.

27
28 The above phenomena could be interpreted in such ways: the higher slurry concentration means
29 the higher PCM mass which led to the increased heat absorption from the PVs modules. As the
30 result, the module's surface temperature was lower and consequently, its heat and power outputs
31 increased and corresponding solar thermal and electrical efficiencies were improved. However,
32 owing to the increased fluid viscosity resulted from the increased slurry concentration, the flow
33 resistance of the slurry across the pipe became higher, leading to the increased pressure drop and

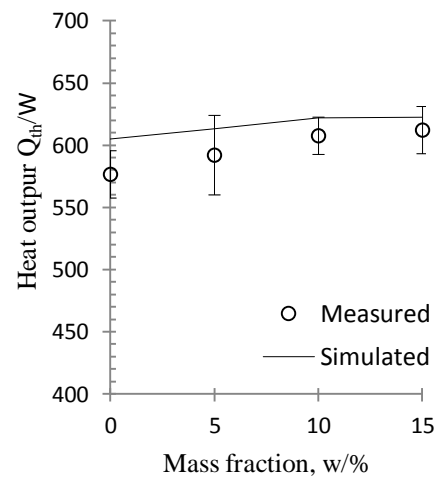
1 pump power output. As a result, the maximum net power output occurred at the 10% of slurry
 2 concentration condition.

3
 4 **Figs 17 to 21** also show the comparisons between the modeling and experimental results under
 5 this set of operational condition. It was found that the U_{max} was in the range 2% to 13% with the
 6 average figure of 7.6% while the root mean square percentage deviation (RMSPE) was below
 7 5.7%. This indicates that the developed theoretical model by the authors [11] could predict the
 8 energy performance of the MPCM slurry based PV/T system at an acceptable accuracy.

9

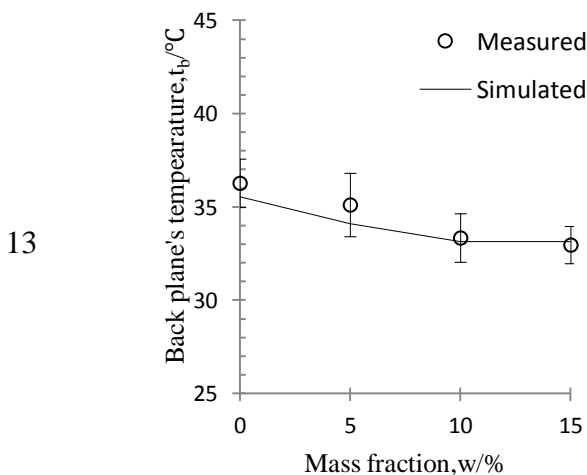


10

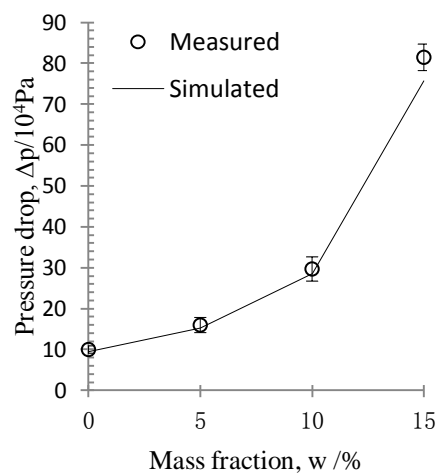


11 Fig.17 Module electricity output vs mass fraction
 12 (RMSPE=1.6%, U_{max} = 2.0%, \bar{U} = 1.5%)

Fig. 18 Module heat output vs mass fraction
 (RMSPE=3.3%, U_{max} = 5.4%, \bar{U} = 3.6%)



13



14 Fig. 19 Module temperature vs mass fraction
 15 (RMSPE=1.9%, U_{max} = 4.8%, \bar{U} = 3.8%)

Fig. 20 Module pressure drop vs mass fraction
 (RMSPE=5.7%, U_{max} = 11.6%, \bar{U} = 8.6%)

16

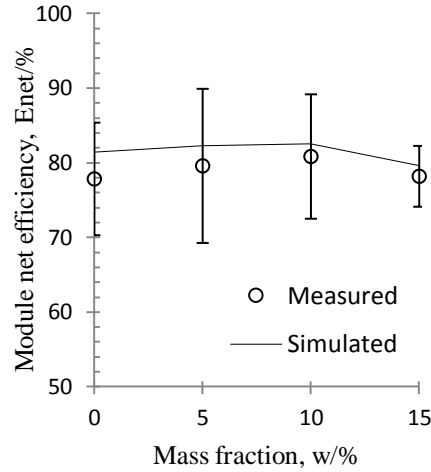


Fig. 21 Module net efficiency vs mass fraction
(RMSPE=3.1%, Umax= 13%, \bar{U} = 7.6%)

5.4 Performance of the PV/T based heat and power system

Under the selected operational condition, i.e. solar radiation of 600 W/m², Reynolds number of 3,000, slurry concentration of 10%, testing was undertaken to evaluate the performance of the overall PV/T based heat and power system. It is found that the heat and power outputs of the PV/T module were 520W and 108W respectively, while the associated solar thermal and electrical efficiencies were 68.8% and 14.1%, giving a 82.9% of overall solar efficiency which is much higher than the average figures of the PVs (10–12% [17]) and solar collectors (40% [18]).

In terms of the overall performance of the integrated system, the net heat output was obtained by using the inlet and outlet temperature of the water from the water tank and the relevant water flow rate, while the net power output should be the figure of the PV power output subtracted by the power consumption of the compressors and pump. By using these figures and definition of the overall coefficient of performance (COP_{sys}), the overall system performance can be preliminarily assessed. The mathematic expression of the COP_{sys} is [19]:

$$COP_{sys} = \frac{Q_{HP,th} + Q_e / 0.38}{Q_{HP,e} + Q_p} \quad (12)$$

Owing to the small heat yield of the PV/T module and low flow rate of the MPCM slurry across the module, difficulties had arisen in selecting the pumps and compressor with the adequate size

1 and capacity. As a consequence, the finally selected pump and compressor were actually oversized;
2 this led to the discouraging results indicating that the PVs' power output (111W) was insufficient
3 to maintain the operation of the compressor and pump which requires around 140 W of power.
4 Even at such an inappropriate operational condition, the system still achieved an overall COP_{sys} of
5 6.95, which was over three times that of the conventional air-source heat pump water heating
6 systems (ASHP) ^[20], and nearly twice that of the solar assisted heat pump systems (ISAHP) ^[21].

8 **6. Conclusions**

9 Based on the published work ^[11] completed by the authors, this paper presented a follow-on
10 research concerning the experimental investigation of the energy performance of a novel PV/T
11 thermal and power system. The system, making use of the Micro-encapsulated Phase Change
12 Material (MPCM) slurry as the working fluid, is composed of a PV/T module, a slurry-to-
13 refrigerant heat exchanger (evaporator), a compressor, a refrigerant-water heat exchanger
14 (condenser), a water tank, an inverter, and other necessary accessories including a slurry pump,
15 valves, an electrical resistance and a controller. The performance of the PV/T module and
16 associated thermal and power system were tested under various solar radiations, slurry Reynolds
17 numbers and PCM concentrations. The test results were compared with the modelling results
18 under the equivalent conditions in order to examine the accuracy of the model prediction. This
19 research has drawn up the following conclusions.

21 The heat and power outputs of the PV/T module increased with the increase of the solar radiation,
22 slurry flow Reynolds number and MPCM concentration. However, the net efficiency varied in the
23 slightly different ways. The solar radiation imposed a negative impact to the efficiencies while the
24 Reynolds number of MPCM concentration imposed the positive impact.

27 Temperature of the PV/T module was a factor directly impacting on its performance. Reduced
28 module temperature could lead to the increased thermal and electrical efficiencies of the module,
29 which could be achieved by imposing a low solar radiation, a high slurry concentration and a large
30 Reynolds number onto the MPCM slurry based PV/T system.

32 Owing to the increased viscosity of the slurry at a higher concentration, the pressure drop of the
33 slurry across the serpentine pipe of the module also grew which led to the increased power

1 consumption of the slurry pump. As a result, the net electrical output of the PV/T module fell
2 when the slurry MPCM concentration increased from 10% to 15%.

3
4 For the benefits of power generation, the MPCM concentration should be controlled to a ratio of
5 10%. At this condition, the net efficiency of the module were in the range 80.8% to 83.9%, which
6 corresponded to the solar radiation of 500 to 700 W/m² and slurry Reynolds number of around
7 3,000. This was considered as the optimum operational performance of the MPCM slurry based
8 PV/T system.

9
10 Parallel comparison between the modelling and experimental results was undertaken under the
11 above indicated operational conditions. The results show that the derivations of the modelling
12 results from the testing data could be controlled to a level of 1.1% to 6.1% (in the RMSPE). This
13 indicates that the model could achieve the reasonable accuracy in predicting the performance of
14 the PV/T system and thus are applicable to the general engineering simulation.

15
16 The overall MPCM slurry applicable PV/T system should be adequately sized to enable achieving
17 the expected energy efficiency and operational performance. Overall, this kind of system is
18 superior to the conventional air-source heat pump water heating systems (ASHP) and solar
19 assisted heat pump systems (ISAHP).

20
21 This research has provided several useful clues on further optimization of such a MPCM slurry
22 based PV/T system, thus helping reduce fossil fuel consumption and carbon emission to the
23 environment globally.

24 **References:**

- 26 [1] Solar Heating and Cooling for a Sustainable Energy Future in Europe (Revised), European
27 Solar Thermal Technology Platform (ESTTP), 2009.
- 28 [2] Technology Roadmap-Solar photovoltaic energy, International Energy Agency, 2010.
29 <http://www.iea-pvps.org>, accessed on 11-04-2011.
- 30 [3] A. Luque, S. Hegedus, Handbook of photovoltaic science and engineering, Wiley, West
31 Sussex, England (2003)
- 32 [4] E. Skoplaki, J.A. Palyvos, On the temperature dependence of photovoltaic module electrical
33 performance: A review of efficiency/power correlations, Solar Energy 2009; 83: 614–624.
- 34 [5] S.C. Solanki, Swapnil Dubey, Arvind Tiwari, Indoor simulation and testing of photovoltaic

- 1 thermal (PV/T) air collectors, *Applied Energy* 2009; 86: 2421–2428.
- 2 [6] Huang B. J et al., Performance evaluation of solar photovoltaic/thermal systems. *Solar*
3 *Energy* 2001; 70: 443-448.
- 4 [7] J. Ji et al., Distributed dynamic modelling and experimental study of PV evaporator in a
5 PV/T solar-assisted heat pump, *International Journal of Heat and Mass Transfer* 2009; 52:
6 1365–1373.
- 7 [8] X Zhang, et al., Review of R&D progress and practical application of the solar
8 photovoltaic/thermal (PV/T) technologies, *Renewable and Sustainable Energy Reviews*
9 2012; 16(01):599-617.
- 10 [9] BASF Factbook 2010, BASF, Ludwigshafen, Germany, 1-20, June 2010.
- 11 [10] Royon L, Guiffant G. Forced convection heat transfer with slurry of phase change material
12 in circular ducts: A phenomenological approach. *Energy Conversion and Management*.
13 2008; 49: 928-32.
- 14 [11] Zhongzhu Qiu, Xudong Zhao*, Peng Li, Xingxing Zhang, Samira Ali. Theoretical
15 Investigation of the Energy Performance of a Novel MPCM Slurry Based PV/T Module.
16 *Energy*. 2015; 87:686-698.
- 17 [12] <http://www.microteklabs.com/index.html>, accessed 08/05/2015.
- 18 [13] Yamagishi Y, Takeuchi H, Pyatenko AT, Kayukawa N. Characteristics of
19 microencapsulated PCM slurry as a heat-transfer fluid. *Aiche Journal*. 1999; 45: 696-707.
- 20 [14] Goel M, Roy SK, Sengupta S. Laminar forced-convection heat transfer in micro-capsulated
21 phase change material suspensions. *International Journal of Heat and Mass Transfer*. 1994;
22 37: 593-604.
- 23 [15] Karaipekli A, Sari A, Kaygusuz K. Thermal conductivity improvement of stearic acid using
24 expanded graphite and carbon fiber for energy storage applications. *Renewable Energy*.
25 2007; 32: 2201-10.
- 26 [16] Sari A, Alkan C, Karaipekli A, Uzun O. Microencapsulated n-octacosane as phase change
27 material for thermal energy storage. *Solar Energy*. 2009; 83: 1757-63.
- 28 [17] Solar photovoltaic modules. <http://www.solardirect.com/pv/pvlist/pvlist.htm>, accessed
29 08/05/2015.
- 30 [18] Solar water heating. <http://bigginhill.co.uk/solar.htm>, accessed 08/05/2015.
- 31 [19] Huang BJ, Lin TH, Hung WC, Sun FS. Performance evaluation of solar
32 photovoltaic/thermal systems. *Solar Energy*. 2001; 70: 443-8.
- 33 [20] Heat pump. https://en.wikipedia.org/wiki/Heat_pump, accessed 08/05/2015.

1 [21] Huang BJ, Chyng JP. Performance characteristics of integral type solar-assisted heat pump.
2 Solar Energy. 2001; 71: 403-14.

3

4 **Acknowledgement**

5 The authors would acknowledge our appreciation to the financial supports from the EU Marie
6 Curie Actions-International Incoming Fellowships (FP7-PEOPLE-2011-IIF-298093).